A New Algorithm for Finding Mixed Layer Depths with Applications to Argo Data and Subantarctic Mode Water Formation*

JAMES HOLTE AND LYNNE TALLEY

Scripps Institution of Oceanography, La Jolla, California

(Manuscript received 15 November 2006, in final form 21 November 2008)

ABSTRACT

A new hybrid method for finding the mixed layer depth (MLD) of individual ocean profiles models the general shape of each profile, searches for physical features in the profile, and calculates threshold and gradient MLDs to assemble a suite of possible MLD values. It then analyzes the patterns in the suite to select a final MLD estimate. The new algorithm is provided in online supplemental materials. Developed using profiles from all oceans, the algorithm is compared to threshold methods that use the C. de Boyer Montégut et al. criteria and to gradient methods using 13 601 Argo profiles from the southeast Pacific and southwest Atlantic Oceans. In general, the threshold methods find deeper MLDs than the new algorithm and the gradient methods produce more anomalous MLDs than the new algorithm. When constrained to using only temperature profiles, the algorithm offers a clear improvement over the temperature threshold and gradient methods; the new temperature algorithm MLDs more closely approximate the density algorithm MLDs than the temperature threshold and gradient MLDs. The algorithm is applied to profiles from a formation region of Subantarctic Mode Water (SAMW) and Antarctic Intermediate Water (AAIW). The density algorithm finds that the deepest MLDs in this region routinely reach 500 dbar and occur north of the A. H. Orsi et al. mean Subantarctic Front in the southeastern Pacific Ocean. The deepest MLDs typically occur in August and September and are congruent with the subsurface salinity minimum, a signature of AAIW.

1. Introduction

The surface layer of the ocean records past winter mixing events and the subsequent onset of spring restratification, as well as the traces of all physical processes occurring above the ocean's permanent thermocline. Typical ocean observations reveal a well-mixed layer, in which temperature, salinity, and density are nearly vertically uniform, embedded in the surface layer. Turbulent mixing processes powered by wind stress and heat exchange at the air–sea interface create this neutrally buoyant and thoroughly mixed column in the upper ocean. This turbulently mixed layer is highly variable. In the summer, mixed layer depths (MLDs) can reach tens of meters or even be absent. In the winter, deep convection driven by surface heat loss can mix the water column to 2000 m in select locations (Marshall and Schott 1999). Coupled with the intense seasonal and spatial variation of the mixed layer is a complexity of structures in the ocean surface layer that can often obscure the depth of the turbulently mixed layer (Sprintall and Roemmich 1999; Dong et al. 2008).

The mixed layer is important to a variety of ocean processes. The mixed layer responds to atmospheric fluxes and transmits those fluxes to the ocean interior. Wind forcing acts through the mixed layer to drive ocean circulation (Chereskin and Roemmich 1991). The depth of the mixed layer establishes the volume of water over which the surface heat flux is distributed (Chen et al. 1994; Ohlmann et al. 1996). In areas where deep convection occurs, winter mixed layer conditions set the properties of the deep and intermediate water masses of the ocean's interior (Talley 1999).

Widespread interest in the processes at work in the mixed layer has spawned numerous arbitrary definitions of the mixed layer, as well as a corresponding number of schemes for finding its depth. Because of the

* Supplemental information related to this paper is available at the Journals Online Web site: http://dx.doi.org/10.1175/2009JTECHO543.1.s1.

Corresponding author address: James Holte, Scripps Institution of Oceanography, 9500 Gilman Drive, Mail Code 0208, La Jolla, CA 92093.
E-mail: jholte@ucsd.edu

DOI: 10.1175/2009JTECHO543.1

paucity of ocean turbulence and mixing measurements, these schemes use temperature and density profiles to find the mixed layer. In these schemes and in this paper, MLD refers to the depth of the uniform surface layer that is assumed to owe its homogeneity to turbulent mixing.

The most widely favored and simplest scheme for finding the MLD is the threshold method. Threshold methods search for the depth at which the temperature or density profiles change by a predefined amount relative to a surface reference value. Kara et al. (2000) and de Boyer Montégut et al. (2004) examined various threshold criteria used in the literature and determined their own optimal global threshold definitions of the MLD. In deciding upon their own criteria, de Boyer Montégut et al. (2004) determined that the larger threshold values commonly used with averaged profiles, such as the 0.5°C threshold value used by Monterey and Levitus (1997) and the 0.8°C used by Kara et al. (2000), overestimated the MLD of individual profiles. Likewise, smaller criteria of 0.1°C underestimated the MLD. After examining numerous profiles, de Boyer Montégut et al. (2004) concluded that 0.2°C was the optimal temperature threshold (TT). They similarly determined an optimal density threshold (DT) value of 0.03 kg m^{-3}. To avoid diurnal heating in the surface layer, de Boyer Montégut et al. (2004) chose a surface reference level of 10 m. These values were recently employed by Oka et al. (2007) in examining the seasonality of the MLD in the North Pacific and by Dong et al. (2008) in examining the mixed layer of the entire Southern Ocean.

Gradient methods, which are also widely used, work much like threshold methods; they assume that there is a strong gradient at the base of the mixed layer and therefore search for critical gradient values (Lukas and Lindstrom 1991). Dong et al. (2008) report that commonly used values range from 0.0005 to 0.05 kg m^{-4} for density gradients (DGs) and 0.025°C m^{-1} for temperature gradients (TGs).

Threshold and gradient methods are limited by their dependence on the surface reference value and the chosen threshold value; it is difficult to decide on a single threshold value or gradient criterion for all ocean profiles. Threshold methods, especially those based solely on temperature, inherently overestimate the MLD. Threshold methods using density falter in density-compensating layers, and those using temperature falter in the presence of salinity barrier layers (Lukas and Lindstrom 1991; Sprintall and Tomczak 1992). Lukas and Lindstrom (1991) found that a density criterion is more reliable for finding the MLD than a temperature criterion, yet there is an order of magnitude fewer density profiles than temperature profiles (Lorbacher et al. 2006).

A variety of more complex methods for finding the MLD have been developed. The ''curvature method'' proposed by Lorbacher et al. (2006) uses conditions for the second derivative and the gradient to identify the MLD. Thomson and Fine (2003) introduced the ''split and merge'' method, which fits a variable number of linear segments to a profile. They found that their method performed similarly to threshold methods. Chu et al. (1999) created a geometric model to determine the MLD of Arctic profiles. Lavender et al. (2002) used the intersection between a straight-line fit to the upper layer and an exponential plus second-order-polynomial fit to the deep layer to estimate the MLD of individual temperature profiles in the Labrador Sea. This method apparently worked in the North Atlantic, but efforts to implement the method in the Southern Ocean did not produce realistic MLDs.

This paper introduces a new algorithm for finding the MLD of individual profiles. The algorithm builds on traditional threshold and gradient methods by tying its estimate of the MLD to physical features in the profile. It accomplishes this by first modeling the profile's general shape; it approximates the seasonal thermocline and the mixed layer with best-fit lines. It then assembles a suite of possible MLD values by calculating the threshold and gradient methods' MLDs, identifying the intersection of the mixed layer and seasonal-thermocline fits (MLTFIT), locating profile maxima or minima, and searching for intrusions at the base of the mixed layer. Finally, it looks for groupings and patterns within the possible MLDs to select the final MLD for each profile. Section 3 details how the algorithm calculates the possible MLDs and selects the final MLD estimate. The algorithm selection criteria were developed through subjective analysis of individual temperature, salinity, and potential-density profiles from all oceans, though the greatest emphasis was placed on the southeast Pacific and southwest Atlantic. The algorithm initially produces a temperature MLD estimate [referred to as the temperature algorithm (TA)]. If the profile also includes salinity, the algorithm subsequently determines the MLDs of the salinity and potential-density profiles. The salinity MLD estimate mainly serves to verify the potential-density MLD estimate [referred to as the density algorithm (DA)] if they are at the same depth. The complete algorithm is provided in online supplemental materials.

Visual examination of the numerous profiles and the algorithm MLDs confirms that the algorithm successfully identifies the MLD. The new algorithm avoids many of the pitfalls of threshold and gradient methods;

the threshold methods overestimate the MLD relative to the other methods and the gradient methods find more anomalous MLDs than the other methods. Section 4 compares the algorithm results to those of standard threshold and gradient methods. For the dataset considered in this paper (introduced in section 2), the temperature algorithm especially improves upon the temperature threshold and gradient methods. Assuming that density MLD estimates are more reliable than temperature MLD estimates (as found by Lukas and Lindstrom 1991), the standard deviations of the differences between the density algorithm MLDs and the three temperature method MLDs can serve as a rough measure of each temperature method's accuracy. The temperature algorithm MLDs nearly match the density algorithm MLDs; the standard deviation of the difference between the temperature algorithm and density algorithm MLDs is 31 dbar, whereas for the temperature threshold and the temperature gradient methods the standard deviation of the differences with the density algorithm MLDs are 62 and 121 dbar, respectively. The density algorithm tends to find slightly shallower MLDs than the density threshold method. The density gradient method finds many anomalous MLDs and is less reliable than either of the other density methods. Preliminary results of applying the algorithms to a larger Southern Ocean dataset (S. Dong 2006, personal communication) generally support the findings from the study region (Dong et al. 2008). The algorithm's greatest utility lies in its ability to find accurate MLDs using only temperature profiles. It can easily be adapted to work with XBT and other temperature-only profiles.

The new algorithm is used to examine Subantarctic Mode Water (SAMW) and Antarctic Intermediate Water (AAIW) formation using Argo data. SAMW is the name given to the waters encompassed by the deep mixed layers immediately north of the Antarctic Circumpolar Current (ACC). AAIW, a subset of SAMW, can be traced as a relatively low-salinity tongue throughout almost all of the Southern Hemisphere and the tropical oceans at about 1000-m depth (Deacon 1937). AAIW is believed to form in the southeast Pacific Ocean, upstream of the Drake Passage (McCartney 1977; England et al. 1993; Talley 1996). The AAIW formation region is a good place to test the algorithm because it features a strong seasonal thermocline in the summer and deep winter mixed layers rivaled only by the North Atlantic, and it is monitored by a collection of Argo floats. The region has been relatively unstudied during the winter. Section 5 discusses the results of applying the algorithm to Argo data from the SAMW–AAIW formation region.

2. Data

This study uses temperature and salinity profiles from 277 profiling floats deployed in the southeast Pacific and southwest Atlantic Oceans as part of the Argo program (Roemmich et al. 2001). In addition, randomly selected profiles from Argo floats in other oceans are used to test the algorithm. Argo is a global observing system of 3000 floats designed to give upper- and middle-layer fields for temperature and salinity of the world's oceans. Argo floats are designed to provide a temperature accuracy of 0.005°C and a salinity accuracy of 0.01 psu.

The region of interest for this study encompasses sections of the southern Pacific and Atlantic Oceans from 40° to 66°S and from 110° to 35°W (Fig. 1). Within this region, Argo floats collected 15 037 profiles between October 2002 and November 2008 (data available online at http://www.usgodae.org/argo/argo.html). In 2002, Canada deployed six floats in the South Pacific and the United Kingdom deployed four floats in the South Atlantic. These floats were supplemented with larger deployments in March 2004 and April 2005. Since 2005, additional deployments and an influx of floats from the growing Argo array have vastly increased the number of profiles in this region. Argo floats typically profile to 2000 m and measure temperature, salinity, and pressure at 70 depth levels. Sample spacing for most floats is less than 20 m to depths of 400 m, below which the spacing increases to 50 m. Figure 2 shows the temperature, potential density, salinity, and sampling interval for a typical Argo profile. The longest float record contained 95 profiles, whereas the shortest contained only 1 profile. All of the profiles included both temperature and salinity data.

Profiles collected before November 2005 were manually examined to remove inconsistencies in temperature, salinity, and pressure. Most floats sampled at regular pressure levels, though the Canadian Argo floats often sampled at irregular pressures and required substantial editing. Float profiles that failed to meet basic quality controls or lacked locations or time stamps were eliminated. Temperature–salinity (T–S) plots allowed the comparison of float data to two World Ocean Circulation Experiment (WOCE) sections: P17E, along 50°S in the southeastern Pacific, and P19C, along 88°W (Tsuchiya and Talley 1998). Except for visually examining the float salinity profiles to confirm that they were largely consistent with the salinity observed during the WOCE cruises, no calibrations of the floats' salinities were performed. This quality-control process trimmed the field to 13 601 profiles. The locations of these profiles are shown in Fig. 1. Potential density was calculated for each profile.

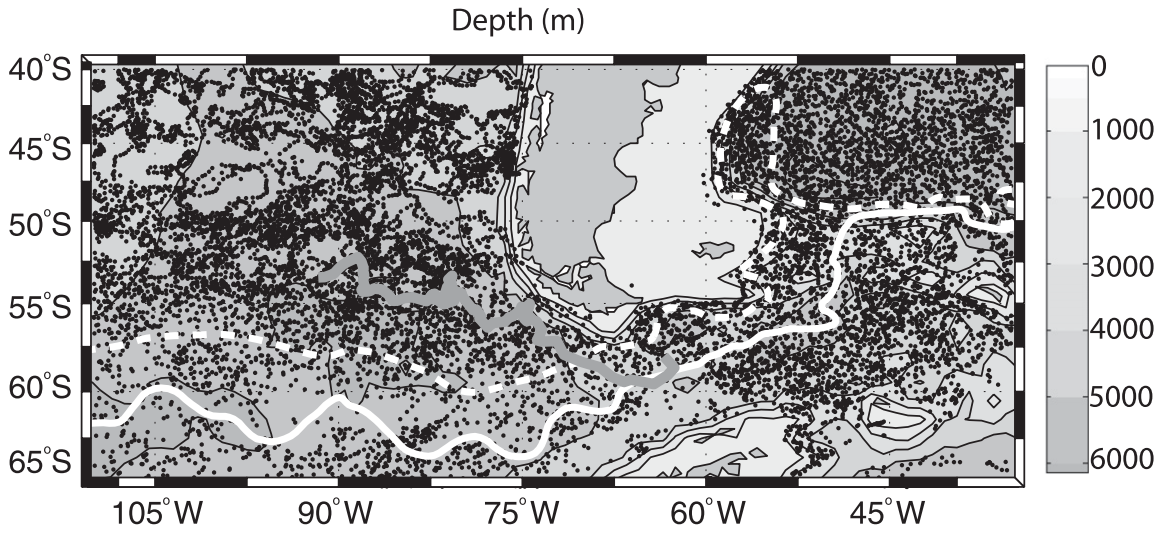

FIG. 1. Profile locations of 277 Argo floats in the South Pacific and Atlantic Oceans. The profiling floats collected 13 601 temperature and salinity profiles between February 2002 and November 2008. The time separation between each float's subsequent profile is 10 days. The study region extends from 40° to 66°S and from 110° to 35°W. The climatological SAF and Polar Front are represented by white and solid lines, respectively (Orsi et al. 1995). The track of float 3900082 is in gray. The bathymetry is contoured at 1000-m intervals.

3. Methodology

This section outlines the algorithm's procedure for finding MLDs. In brief, the algorithm models the profile's general shape, calculates a suite of possible MLD values, and then looks for groupings and patterns within the possible MLDs to select the final MLD estimate for each profile. It does this separately for each temperature, salinity, and potential-density profile to produce final MLD estimates for the temperature and potential-density profiles. The temperature algorithm is detailed in this section because it offers a substantial improvement over its threshold and gradient counterparts. The salinity and potential-density algorithms work in a similar fashion. The entire algorithm is supplied in online supplemental materials. The following description of the temperature algorithm is divided into three parts: first, a description of how the algorithm calculates the five possible MLD values; second, an explanation of how the algorithm selects the final MLD estimate from the pool of possible MLDs; and third, an example.

a. Assembling the possible MLD values

Examples of typical summer and winter profiles are shown in Fig. 3, as well as the five possible MLD values that the temperature algorithm calculates for each profile. For temperature profiles, the five possible MLD measures are the MLTFIT, the temperature maximum (TM), the temperature gradient MLD estimate (DTM), nearly collocated temperature and temperature gradient maxima (TDTM; this represents intrusions at the base of the mixed layer), and the temperature threshold MLD estimate (TTMLD). For reference, the five possible MLD values for temperature are listed in Table 1. For salinity, the possible MLD values are the density threshold MLD estimate, the salinity minimum, the salinity gradient extreme, collocated salinity and salinity gradient minima (representing an intrusion at the base of the mixed layer, if one exists), the intersection of the salinity mixed layer and thermocline fits, and the final temperature algorithm MLD. For density, the algorithm uses the density threshold MLD estimate, the density gradient MLD estimate, and the intersection of the density mixed layer and thermocline fits, as well as the temperature threshold MLD estimate, collocated

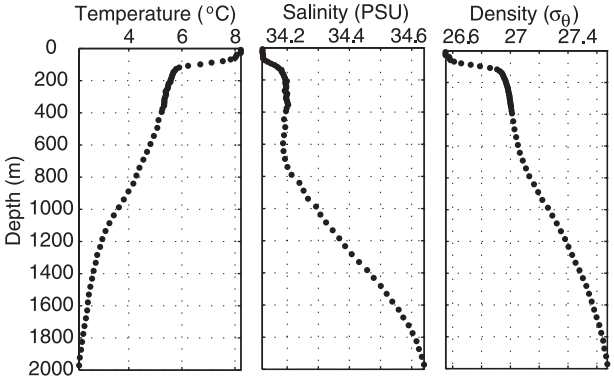

FIG. 2. Example Argo profiles of temperature, potential density, and salinity to 2000 m from float 3900082 on 29 Jan 2003 at 52.7°S, 89.7°W. To 400 m, the float's sampling interval is 10 m, after which it increases to 50 m. This profile is from a Canadian Argo float.

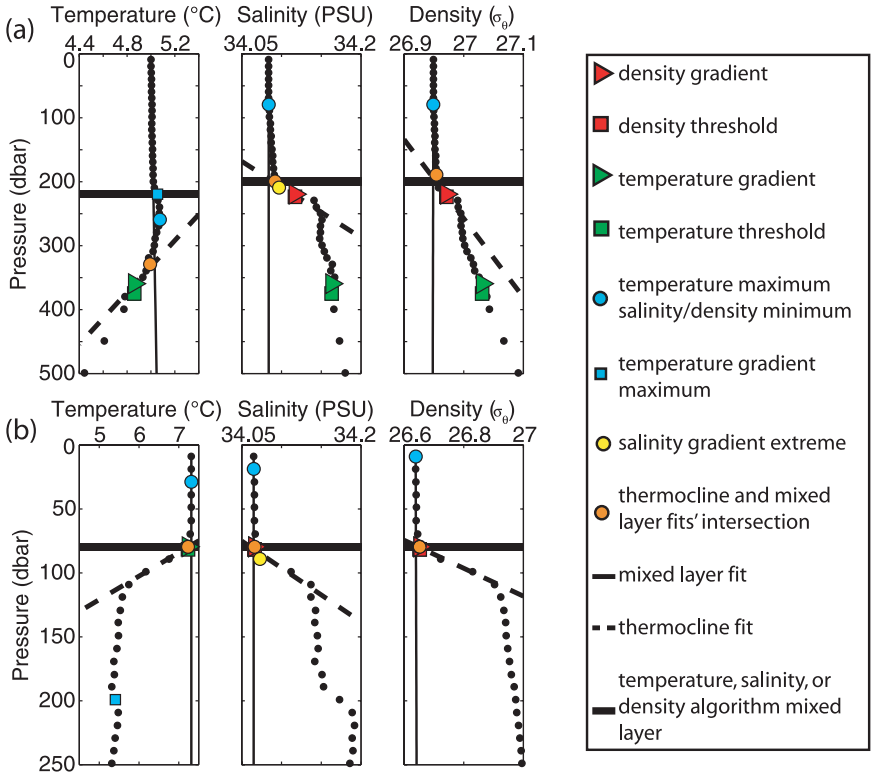

FIG. 3. Temperature, salinity, and potential-density profiles (black dots) collected by float 3900085 in (a) winter and (b) summer. The winter profile was collected on 12 Jul 2003 in the South Pacific Ocean at 54.3°S, 87.8°W. The summer profile was collected on 12 Feb 2003 at 52.6°S, 89.4°W. The algorithm identifies a unique MLD for each temperature, salinity, and density profile (horizontal bold solid lines). The temperature algorithm does not use the density threshold MLD. The algorithm mixed layer (thin solid line) and thermocline (dashed line) fits are also plotted. The five mixed layer estimates used in the temperature algorithm's selection process are the MTLFIT (orange circle), TM (light blue circle), DTM (green triangle; criterion of 0.005°C dbar^{-1}), collocated TDTM (located at the temperature gradient maxima; light blue square), and TTMLD [green square; de Boyer Montégut et al.'s (2004) threshold of 0.2°C]. For the density and salinity profiles, the threshold density MLD [red square; de Boyer Montégut et al.'s (2004) threshold of 0.03 kg m^{-3}] and the gradient density MLD (red triangle; criterion of 0.0005 kg m^{-3} dbar^{-1}) are plotted for each profile. The light blue circles correspond to profile minima and the yellow circle corresponds to the salinity gradient extreme.

temperature and temperature gradient maxima, the temperature maximum, and the final MLDs from the temperature and salinity algorithms.

The algorithm derives its five possible MLD values for temperature as follows:

1) The algorithm initially uses a simple threshold method to find the approximate MLDs of the temperature and potential-density profiles. Starting at the surface, threshold methods search progressively deeper levels until they find a level where the temperature or potential density differs from the surface reference value by a specified threshold. To calculate TTMLD, the algorithm looks for the minimum depth at which $|T(p) - T(p_o)| \geq \Delta T_t$, where T is the temperature, p is the pressure, p_o is the reference pressure, and ΔT_t is the temperature threshold. The algorithm linearly interpolates the temperature profile between Argo measurements to find the depth that exactly matches the threshold criterion. For potential density, the algorithm implements the same procedure but uses the potential-density anomaly σ_θ. Following de Boyer Montégut et al. (2004), 0.2°C and 0.03 kg m^{-3} are used as the threshold difference criteria and the Argo measurement closest to 10 dbar is used as the surface reference value.
2) The algorithm then calculates the temperature, salinity, and potential-density gradients using a difference formula. For calculating the temperature gradient, the algorithm uses

TABLE 1. Acronyms for the temperature algorithm's five possible MLDs.

MLTFIT	Intersection of mixed layer and thermocline fits
TM	Temperature maximum
DTM	Temperature gradient MLD estimate
TDTM	Collocated temperature and temperature gradient maxima
TTMLD	Temperature threshold MLD estimate

$$\frac{\partial T_i}{\partial p_i} = \frac{T_i - T_{i+1}}{p_i - p_{i+1}}, \tag{1}$$

where i is the depth measurement index from the surface ($i = 1$) to one level above the bottom of the profile ($i = n - 1$). The algorithm first uses the gradient to calculate gradient MLDs for temperature and potential density; it finds the depth at which the temperature and potential-density gradients exceed specified gradient criteria. Following Dong et al. (2008), the algorithm uses a potential-density gradient criterion of 0.0005 kg m^{-3} $dbar^{-1}$. It uses a temperature gradient criterion of 0.005°C $dbar^{-1}$. This criterion was found to better approximate the MLD than larger criteria. For temperature, the algorithm looks for the depth at which $|\partial T(p)/\partial p| \geq$ 0.005°C $dbar^{-1}$. If these gradient criteria are not met, the algorithm takes the depth of the maximum of the gradient's absolute value as the gradient MLD. To aid in identifying persistent change in each of the variables (such as the thermocline, which is identified in step 4), the algorithm then smoothes the gradient with a three-point running mean to eliminate small vertical-scale spikes and small-scale intrusions.

3) The algorithm fits a straight line to the mixed layers of the temperature, salinity, and potential-density profiles. Starting at the surface, the algorithm uses the first two points of the profile to calculate a straight-line least squares fit to the mixed layer. It increases the depth and the number of points used in the fit until it reaches the bottom of the profile. For each fit, the algorithm calculates the error by summing the squared difference between the fit and the profile over the depth of the fit. For temperature, this is expressed as

$$E_i = \sum_{j=1}^{i} (T(j) - T_{\mathrm{MLfit}_i}(j))^2. \tag{2}$$

In this example, E_i is the error for the ith fit (extending to depth index i), T_{MLfit_i} is the straight-line temperature fit, and i indexes the depth of the fit and the fit itself. There is a different error and fit for each i.

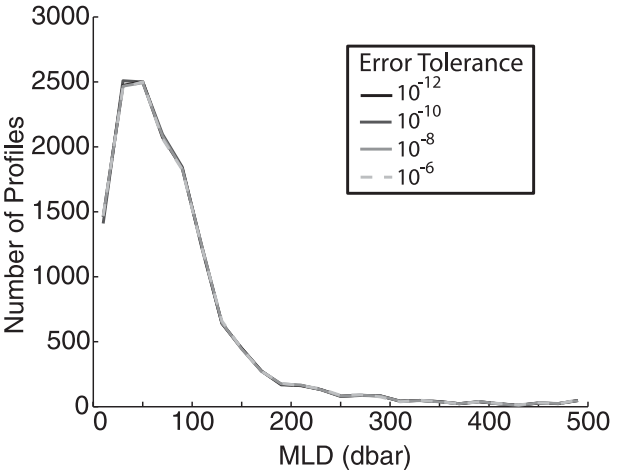

FIG. 4. Distribution of MLDs for the temperature algorithm with varying error tolerances of 10^{-6} (dashed gray), 10^{-8} (light gray), 10^{-10} (dark gray), and 10^{-12} (black). An error tolerance of 10^{-10} was chosen for the algorithm.

The algorithm only sums the error over the depth of the fit, so a straight-line fit no longer accurately describes the profile as the depth of the fit increases past the mixed layer and as the error increases. The algorithm normalizes the errors by dividing each E_i by the total sum of the errors. The normalized error E_{i_n} is given by

$$E_{i_n} = \frac{E_i}{\sum_{i=2}^{n} E_i}. \tag{3}$$

Normalizing the error removes dependence on the magnitude of the seasonal thermocline and produces a unitless error. The algorithm takes the deepest mixed layer fit that satisfies a specified error tolerance, $E_T = 10^{-10}$. This small error tolerance is used to ensure that the mixed layer fit closely matches the mixed layer and does not use any points in the seasonal thermocline; it consistently produces a straight-line fit to the mixed layer and results in the average use of 3.5 Argo measurements per mixed layer fit. Varying the error tolerance has little effect on the MLDs found by the algorithm (Fig. 4).

4) Straight lines are fit to the seasonal thermoclines of each temperature, salinity, and potential-density profile. The algorithm later finds the intersection of the thermocline and mixed layer fits as one possible measure of the MLD. The algorithm identifies the center of the seasonal thermocline for each profile as the depth of the maximum of the absolute values of the smoothed temperature, salinity, and potential-density gradients (calculated in step 2). For temperature, this is expressed as

$$i_{\text{therm}} = \left|\frac{\partial T_i}{\partial p_i}\right|_{\max}, \tag{4}$$

where i_{therm} is the depth index of the thermocline. It is quite successful in the summer, when the seasonal thermocline is easily identifiable as a large spike in the dT/dp, dS/dp, and $d\sigma_\theta/dp$ profiles. The algorithm uses i_{therm} and the two neighboring points ($i_{\text{therm}} - 1$ and $i_{\text{therm}} + 1$) to fit a straight line to the seasonal thermocline. Because Argo floats record few data points in the thermocline, including more than three points in the fit skews the thermocline vertically.

5) The algorithm assembles the possible values of the MLD for each temperature, salinity, and potential-density profile. The five possible MLD values for the temperature algorithm are given in (i)–(v).

   (i) The first possible MLD is from the TTMLD calculation. This is represented as

$$p(T = T_o \pm 0.2°\text{C}), \tag{5}$$

   where T_o is the surface reference temperature. The salinity and density algorithms use the density threshold, $p(\sigma\theta = \sigma_{\theta_o} + 0.003 \text{ kg m}^{-3})$, where σ_{θ_o} is the surface reference potential density.

   (ii) The second MLD value for temperature is the result of the DTM calculation. This is represented as

$$p\left(\left|\frac{\partial T}{\partial p}\right| > 0.005°\text{C dbar}^{-1}\right). \tag{6}$$

   If the gradient criterion is not met, the algorithm takes the gradient extreme,

$$p\left(\left|\frac{\partial T}{\partial p}\right|_{\max}\right). \tag{7}$$

   The potential-density gradient MLD is calculated in the same manner, using a criterion of 0.0005 kg m^{-3} dbar^{-1}. The salinity algorithm uses the salinity gradient extreme.

   (iii) The algorithm then finds the depth of the TM and the salinity and density minima. For temperature, this is represented as

$$p(T_{\max}). \tag{8}$$

   (iv) For the fourth possible MLD value, the algorithm searches for a specific feature in the profile. Surface cooling and intense wind events in the winter deepen the mixed layer and erode the summer thermocline. This process often leaves subsurface anomalies of temperature or salinity at the base of the mixed layer. An example of this feature is shown in Fig. 3a. The algorithm identifies these features in temperature profiles by searching for maxima of the smoothed temperature gradient profiles within a specified distance (the parameter ΔD) of subsurface TM; the algorithm takes the shallowest of the two as the fourth possible MLD value (TDTM). This is represented as

$$p\left[\left(\frac{\partial T}{\partial p}\right)_{\max}, T_{\max}\right]_{\min} \quad \text{if} \quad \left|p\left[\left(\frac{\partial T}{\partial p}\right)_{\max}\right] - p(T_{\max})\right| \le \Delta D. \tag{9}$$

   The fourth possible MLD value is set to zero if the temperature and temperature gradient maxima are separated by more than ΔD:

$$0 \quad \text{if} \quad \left|p\left[\left(\frac{\partial T}{\partial p}\right)_{\max}\right] - p(T_{\max})\right| > \Delta D. \tag{10}$$

   Figure 3a provides an example of a subsurface temperature anomaly where TM and the temperature gradient maximum are separated by 50 dbar. Setting ΔD, the maximum allowable separation between TM and temperature gradient maxima, to 100 dbar allows the algorithm to identify temperature intrusions at the base of the mixed layer. As shown in Fig. 5, this value of ΔD encompasses the profusion of deep MLDs

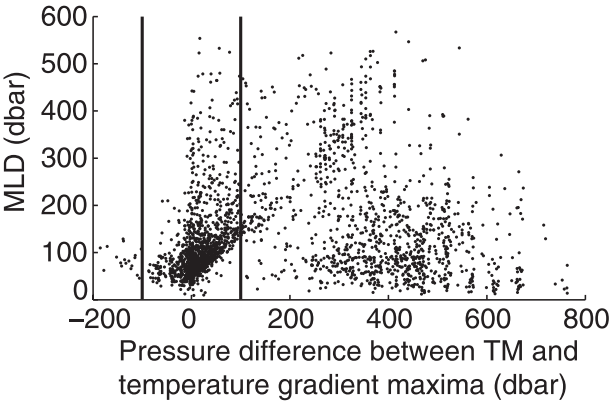

FIG. 5. Pressure difference between the depth of the temperature maxima and the temperature gradient maxima ($p(TM) - p[(\partial T/\partial p)_{\max}]$) plotted against the MLD as determined by the density threshold method. Only values for subsurface temperature maxima or temperature gradient maxima are plotted. The vertical lines denote pressure differences of ∓ 100 dbar.

scattered around 0.0 dbar separation between TM and the temperature gradient maximum.

(iv) The final possible MLD value represents another physical feature in the profile; the depth of MLTFIT. This is designed to capture the MLD in profiles with homogenous mixed layers near the surface and strong seasonal thermoclines. For temperature, this is represented as

$$p(T_{\text{MLfit}} = T_{\text{Thermfit}}), \tag{11}$$

where T_{MLfit} is the mixed layer fit and T_{Thermfit} is the seasonal-thermocline fit. MLTFIT is set to 0 if the fits do not intersect. The salinity and density algorithms use their respective fits. This MLD measure works especially well in the summer, when the algorithm can easily identify the seasonal thermocline, but occasionally falters in the winter, when the seasonal thermocline is weak.

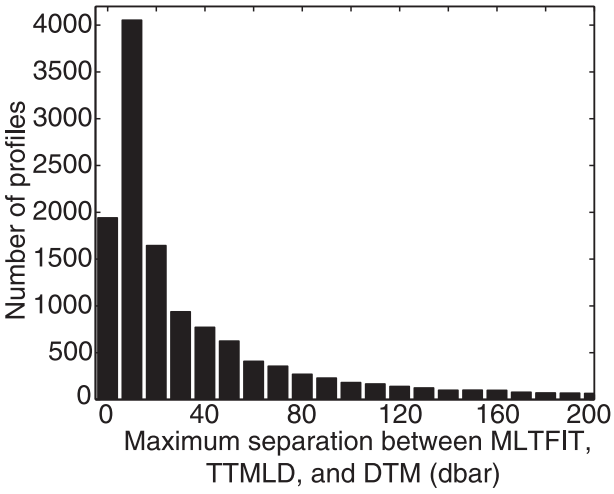

FIG. 6. Distribution of the maximum separation between MLTFIT, TTMLD, and DTM [(|TTMLD − DTM|, |MLTFIT − DTM|, and |TTMLD − MLTFIT|)$_{\max}$]. The bin width is 10 dbar, so the first bin, centered at 0-dbar separation, includes all profiles in which these MLD estimates are separated by a maximum of 5 dbar.

b. Selecting the MLD estimate

The algorithm selection process is divided into two parts. In summary, the algorithm first determines whether the profile resembles a summer or winter profile. Simplistically, a summer profile generally consists of a homogenous mixed layer near the surface; a seasonal thermocline where the temperature, salinity, and density change abruptly with depth; and a deep-water layer that is seasonally invariant. Winter profiles lack the strong summer thermocline; the mixed layer visually blends into the underlying waters. The algorithm's initial MLD selection is dependent on the ''type'' of profile. Then, over a series of steps, the algorithm examines the other possible MLD values, looks for clusters of possible MLD values, and either confirms or replaces the initial MLD selection. The algorithm selects MLDs for each temperature and potential-density profile; the algorithm also selects a salinity MLD, but it only serves to verify the potential-density MLD. The temperature algorithm's selection process is outlined in the following steps:

1) Before the algorithm can search for clusters of the possible MLDs, it must first define a depth range over which to search. The possible MLDs are rarely at the same Argo depth levels but might be within 15 dbar of each other; this range parameter r allows the algorithm to identify clusters of possible MLDs separated by less than r and to accommodate Argo's sampling scheme. The algorithm also avoids selecting temperature maxima at the surface by checking whether they are deeper than r. The distribution of the maximum separation between MLTFIT, TTMLD, and DTM (plotted in Fig. 6) determines the value of r. MLTFIT, TTMLD, and DTM have maximum separations of 5 dbar for 1941 profiles, 5–15 dbar for 4054 profiles, and 15–25 dbar for 1645 profiles. Because there is a falloff in the number of profiles with maximum separations greater than 25 dbar, r is set to 25 dbar, the approximate equivalent of two Argo depth bins.
2) The algorithm uses the temperature or potential-density changes across the thermocline (ΔT and $\Delta\sigma_\theta$) to estimate whether a profile is summer-like (strong thermocline beneath the mixed layer) or winter-like (weak thermocline beneath the mixed layer). The temperature change across the thermocline, in terms of Argo depth bins, is defined as $T(i_{\text{MLTFIT}}) - T(i_{\text{MLTFIT}} + 2)$, where i_{MLTFIT} is the Argo depth index of MLTFIT; the potential-density change is calculated in the same manner. The algorithm compares this temperature change to a third parameter ΔT_c a temperature change cutoff, for information about the strength of the seasonal thermocline and to decide if a profile is summer- or winter-like. Figure 7 plots the temperature and potential-density changes across the thermocline against the MLD as well as the temperature-change and potential-density-change cutoffs. If the temperature change is within the cutoff region ($0.5°\text{C} > \Delta T > -0.25°\text{C}$), then the algorithm initially assumes that the profile is winter-like. The potential-density-change cutoff σ_{θ_c} is -0.06 kg m^{-3} ($\Delta\sigma_\theta > -0.06$ kg m^{-3} for winter-like profiles). In the

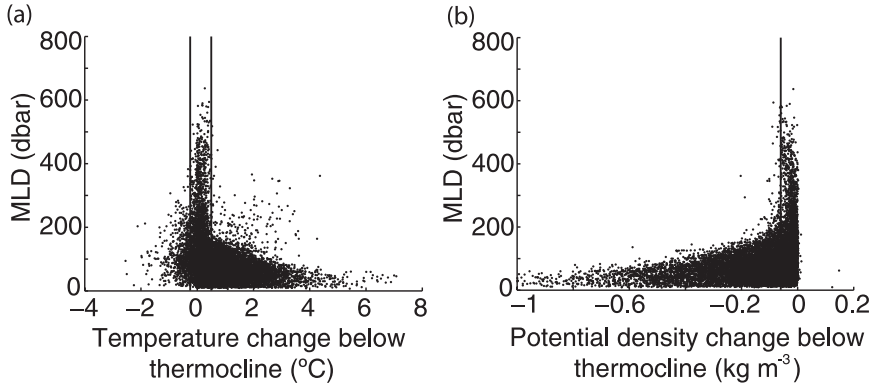

FIG. 7. (a) The temperature change across the thermocline, ΔT, is plotted against MLD. (b) Same as in (a), but for potential density. In both cases the MLD was found using the density threshold method. The vertical lines correspond to the temperature-change and potential-density-change cutoffs. The temperature-change cutoffs are 0.5° and −0.25°C. The potential-density-change cutoff is -0.06 kg m^{-3}. Temperature changes within the temperature cutoffs and potential-density changes greater than the potential-density cutoff are treated as winter-like profiles by the algorithm.

study region, 83% of profiles with MLDs deeper than 200 dbar are within the temperature-change cutoff range; 90% of the profiles with MLDs deeper than 200 dbar are within the potential-density-change cutoff.

3) If ΔT falls outside of the winter cutoff (ΔT_c), the algorithm initially assumes that the profile features a strong thermocline. Figure 8 shows the temperature algorithm flow path for these summer-like profiles. Because summer-like profiles are assumed to feature strong thermoclines, the algorithm first assigns MLTFIT to the final MLD. Steps (i) and (ii) check the other possible MLDs to ensure that this MLD assignment is reasonable; if not, the MLD is reassigned to one of the other possible MLDs as described.

   (i) Profiles with multiple temperature inversions, such as polar profiles, often have shallow MLDs but lack identifiable seasonal thermoclines. These profiles can cause the algorithm to misidentify the thermocline and thus confound MLTFIT. To identify these profiles, in Fig. 8a, the algorithm searches for temperature increases beneath the mixed layer ($\Delta T < 0$) and checks whether MLTFIT overestimated the MLD relative to TTMLD. If so, the algorithm assigns the MLD to TTMLD.

   (ii) This step treats TTMLD as an upper bound on the MLD to evaluate MLTFIT and TM. The algorithm first tests the current MLD against TTMLD (Fig. 8b); the final MLD is assigned to the current MLD if it is shallower than TTMLD. If the current MLD is deeper than TTMLD, the algorithm subsequently examines TM. If TM is beneath the surface and shallower than TTMLD, then the algorithm assigns the MLD to TM; if not, then it assigns the MLD to TTMLD (Fig. 8c).

4) If ΔT is within the winter cutoff range, the temperature algorithm assumes that the profile is winter-like and follows the flow path shown in Fig. 9. The selection process is conducted in the following steps:

   (i) The algorithm first tests whether it identified a seasonal thermocline (and therefore a meaningful

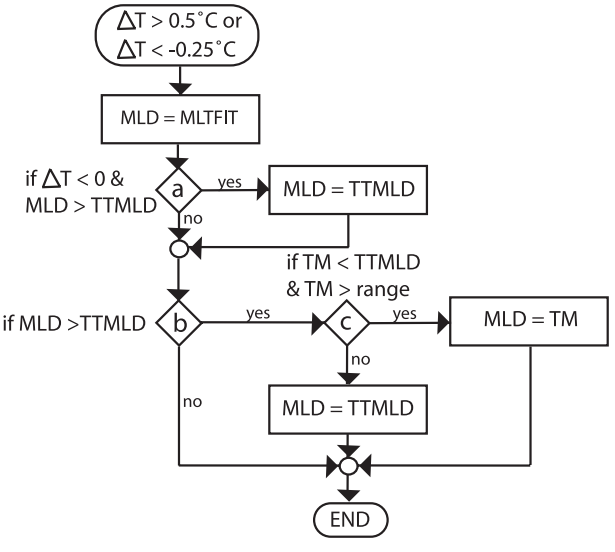

FIG. 8. The temperature algorithm's summer flow diagram.

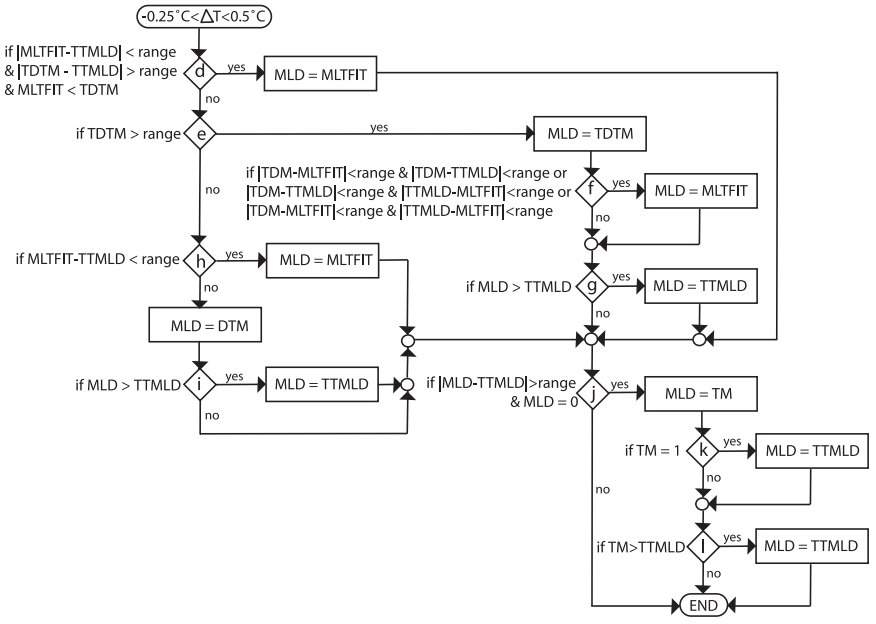

FIG. 9. The temperature algorithm's winter flow diagram.

MLD value for MLTFIT) by checking if MLTFIT and TTMLD are in close proximity ($|\text{MLTFIT} - \text{TTMLD}| < r$) and by comparing MLTFIT to TDTM. TDTM represents a subsurface temperature anomaly at the base of the mixed layer, if such an anomaly exists. When the algorithm fails to identify a seasonal thermocline, it often instead identifies the permanent thermocline, producing a very deep estimate for MLTFIT. Therefore, if MLTFIT is shallower than TDTM and if TDTM and TTMLD differ by more than r, the algorithm has most likely identified the seasonal thermocline, so the MLD is assigned to MLTFIT (Fig. 9d) and the algorithm proceeds to (iv).

(ii) If the algorithm did not capture the seasonal thermocline (the MLD was not assigned to MLTFIT), then the algorithm searches for temperature anomalies at the base of the mixed layer; if TDTM exists and is not at the surface, the algorithm assigns the MLD to TDTM (Fig. 9e). It then checks that TDTM does not greatly differ from the other possible MLDs (Figs. 9f,g). It accomplishes this by first searching for clusters of three other MLD estimates; it determines if any two sets of MLTFIT, TTMLD, and DTM ($|\text{MLTFIT} - \text{TTMLD}|$, $|\text{MLTFIT} - \text{DTM}|$, or $|\text{DTM} - \text{TTMLD}|$) are separated by less than r, as they often are for profiles with seasonal thermoclines. If so, the MLD is assigned to MLTFIT (Fig. 9f). As a final check, if the MLD is deeper than TTMLD, the MLD is reassigned to TTMLD in Fig. 9g. The algorithm then proceeds to (iv).

(iii) Convective winter mixing does not necessarily produce temperature anomalies at the base of the mixed layer, so TDTM does not necessarily exist. Figures 9h,i are evaluated if TDTM does not exist and if the algorithm did not assign the MLD to MLTFIT. The algorithm again considers MLTFIT by comparing MLTFIT to TTMLD; if MLTFIT is not more than r deeper than TTMLD ($\text{MLTFIT} - \text{TTMLD} < r$; Fig. 9h), the MLD is assigned to MLTFIT. If MLTFIT is more than r deeper than TTMLD, the MLD is assigned to the gradient MLD estimate, DTM. To test DTM, the algorithm checks whether it is deeper than TTMLD (Fig. 9i). If DTM is deeper than TTMLD, the MLD is reassigned to TTMLD.

(iv) The algorithm checks for poor thermocline fits by testing whether the final MLD estimate has been assigned to the surface and whether this near-surface MLD differs from TTMLD ($|\text{MLD} - \text{TTMLD}| < r$). If these conditions are met, the MLD is most likely shallow and the algorithm assigns the MLD to TM (Fig. 9j). In two final checks, the algorithm assigns the MLD to TTMLD if TM is at the surface or if it is deeper than TTMLD (Figs. 9k,l).

c. Example selection processes

Figure 3a provides an example of the temperature algorithm's selection process. The algorithm first compares the temperature change below MLTFIT to the temperature-change cutoff ΔT_c. For this profile, $\Delta T = 0.06$°C, so the algorithm considers this a winter-like profile and follows the path in Fig. 9. MLTFIT is deeper than TDTM (Fig. 9d), so the algorithm looks for a subsurface temperature maximum at the base of the mixed layer (Fig. 9e); TDTM is greater than r, so the algorithm assigns the MLD to TDTM. In Fig. 9f, the algorithm checks whether there might be a thermocline, but MLTFIT is 100 dbar shallower than TTMLD. TDTM is also much shallower than TTMLD (Fig. 9g), so the final MLD is assigned to TDTM. From visual inspection of the salinity and potential-density profiles, it is clear that the temperature algorithm MLD is closer to the actual MLD than the temperature threshold and temperature gradient MLDs.

Figure 3b provides another example. This profile has a strong seasonal thermocline ($\Delta T = 1.4$°C), so the algorithm considers this a summer-like profile and initially assigns the MLD to MLTFIT. MLTFIT is at the same depth as TTMLD, so the MLD assignment does not change.

For the temperature profiles in this study, the algorithm uses the intersection of the mixed layer and thermocline fits as the MLD for 58% of the profiles in the study region. The threshold MLD is used for 22% of the profiles and the gradient MLD is used for 9%. Collocated temperature and temperature gradient maxima are used for 7% of the profiles and temperature maxima are used for 4%.

4. Comparison to other methods

The MLDs produced by six different methods are considered here to evaluate the algorithm. The six MLD estimates are 1) the temperature algorithm estimate, 2) the density algorithm estimate, 3) a temperature threshold estimate (threshold of 0.2°C), 4) a density threshold estimate (threshold of 0.03 kg m^{-3}), 5) a temperature gradient estimate (criterion of 0.005°C $dbar^{-1}$), and 6) a density gradient estimate (criterion of 0.0005 kg m^{-3} $dbar^{-1}$). The threshold estimates are from de Boyer Montégut et al. (2004) and the gradient criteria are derived from Dong et al. (2008). We evaluate the six methods by first examining their MLDs for a single profile and then a single float record. For the float record, the exact MLD was determined by visually identifying the homogenous mixed layer and comparing it to the MLD estimates of the six methods. The analysis is then expanded to the distribution of MLDs for all of the profiles in the southeast Pacific and southwest Atlantic. The algorithm and threshold MLD distributions for the entire Southern Ocean are briefly examined.

a. Individual profile comparison

The algorithm MLDs are first compared to threshold and gradient MLDs for the two sets of temperature and potential-density profiles in Fig. 3. For the winter profile (Fig. 3a), the algorithm calculates MLDs of 220 dbar for temperature and 200 dbar for potential density. The temperature threshold ($\Delta T = 0.2$°C) calculates an MLD of 375 dbar; the density threshold ($\Delta\sigma_\theta = 0.03$ kg m^{-3}) calculates an MLD of 225 dbar. The temperature gradient method (criterion of 0.005°C $dbar^{-1}$) identifies an MLD of 360 dbar, and the density gradient method (criterion of 0.0005 kg m^{-3} $dbar^{-1}$) identifies an MLD of 220 dbar. The temperature algorithm seizes upon the close proximity of the temperature maximum and the temperature gradient maximum to identify the MLD [Eq. (9) represents the MLD]. The temperature threshold and temperature gradient methods both overestimate the MLD by nearly 150 dbar. In general, winter profiles, with no strong, sustained gradients in density or temperature below the mixed layer, prove difficult for the temperature threshold and gradient methods. The density threshold and gradient methods slightly overestimate the MLD compared to the density algorithm.

For the summer profile (Fig. 3b), the algorithm calculates MLDs of 80 dbar for both temperature and potential density using the intersection between the thermocline and mixed layer fits [represented by Eq. (11)]. All of the threshold and gradient methods find similar MLDs, though the threshold MLDs are slightly deeper. These MLDs are representative of typical results. In general, the algorithm, threshold, and gradient methods produce similar summer MLDs; the strong seasonal thermocline and pycnocline prohibit the threshold and gradient methods from advancing very far below the actual MLD and ensure that the algorithm identifies and fits the thermocline.

b. Individual float comparison

Having examined two profiles, the comparison between the algorithm, threshold, and gradient methods is expanded to an entire float record. Figure 10 presents the track of float 3900082. The float was deployed in December 2002, off the coast of Chile in the southeast Pacific Ocean. It collected 95 profiles before it ceased transmitting in August 2005. Entwined in numerous eddies, it crossed the ACC and was carried through the Drake Passage and into the polar ocean surrounding Antarctica. The potential-density time series of float

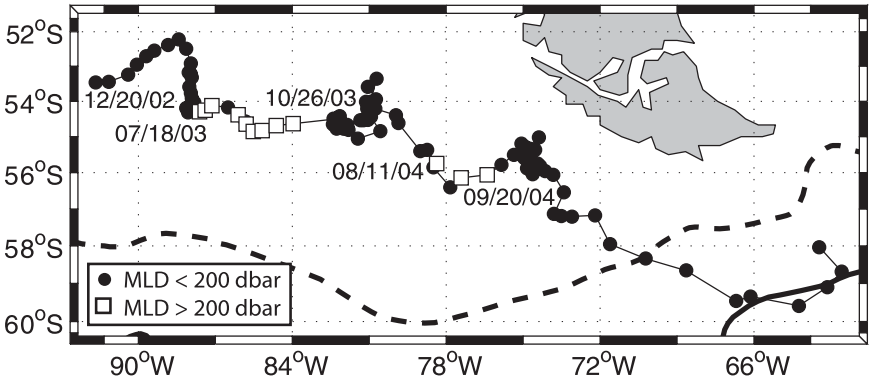

FIG. 10. Track of Argo float 3900082. The float was deployed in the Pacific Ocean off Chile at 53.5°S, 91.7°W in December 2002 and has since passed through the Drake Passage. Profiles with mixed layers deeper than 200 dbar are represented by open squares (MLD calculated by the density algorithm). The first period of deep mixed layers lasted from 18 Jul to 26 Oct 2003; the second lasted from 11 Aug to 20 Sep 2004. The SAF and Polar Front are represented by the dashed and solid lines (Orsi et al. 1995).

3900082 is plotted in Fig. 11a, in addition to three MLD time series. Figure 11b is the temperature time series of the float, again in addition to three MLD time series.

The density algorithm, threshold, and gradient methods generally produce comparable MLDs in summer (Figs. 3b, 11a). Subtle gradients in temperature, salinity, and density that blend mixed layers into deep waters, as well as a wide variety of subsurface features such as salinity intrusions, often obscure the MLD of winter profiles. The density threshold winter MLDs are generally deeper than the density algorithm winter MLDs (Fig. 11a). As seen in Fig. 3a, weak density gradients at the base of the mixed layer cause the density threshold method to slightly overestimate the MLD in winter. The density gradient is much more erratic than the other methods, as evidenced by its frequent jumps to both shallow and extraordinarily deep MLDs in Fig. 11a. In winter 2004, the density gradient method estimates

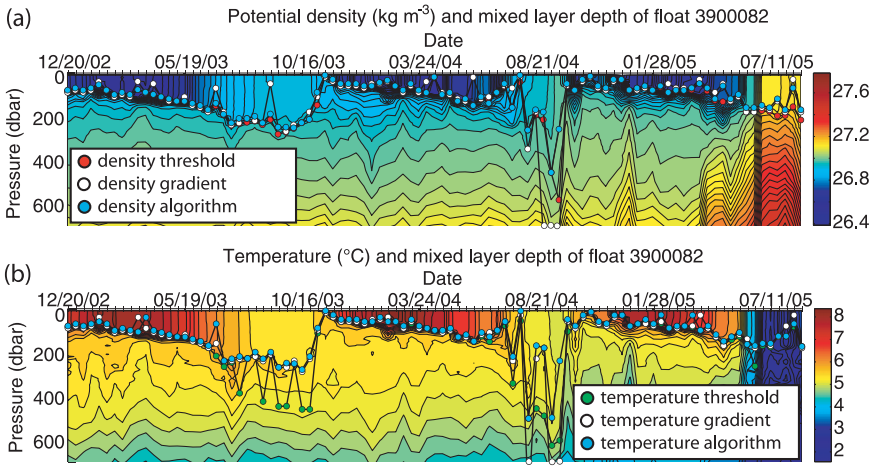

FIG. 11. Time series of (a) potential density and (b) temperature for float 3900082. The profiles extend to 2000 dbar but are only shown to 700 dbar. The time series runs from December 2002 to August 2005; the tick marks along the time axis denote 10-day profile separation. In (a), the contour intervals are 0.02 kg m^{-3} and three MLD time series are plotted: the density threshold calculation, using de Boyer Montégut et al.'s (2004) criterion (red circle); the density gradient calculation (white circle), using a criterion of 0.0005 kg m^{-3} $dbar^{-1}$; and the density algorithm's result (light blue circle). Solid lines connect each MLD time series. In (b), the contour interval is 0.2°C, the temperature threshold is plotted in green (criterion of de Boyer Montégut et al. 2004), the temperature gradient result is plotted in white (criterion of 0.005°C $dbar^{-1}$), and the temperature algorithm result is plotted in light blue.

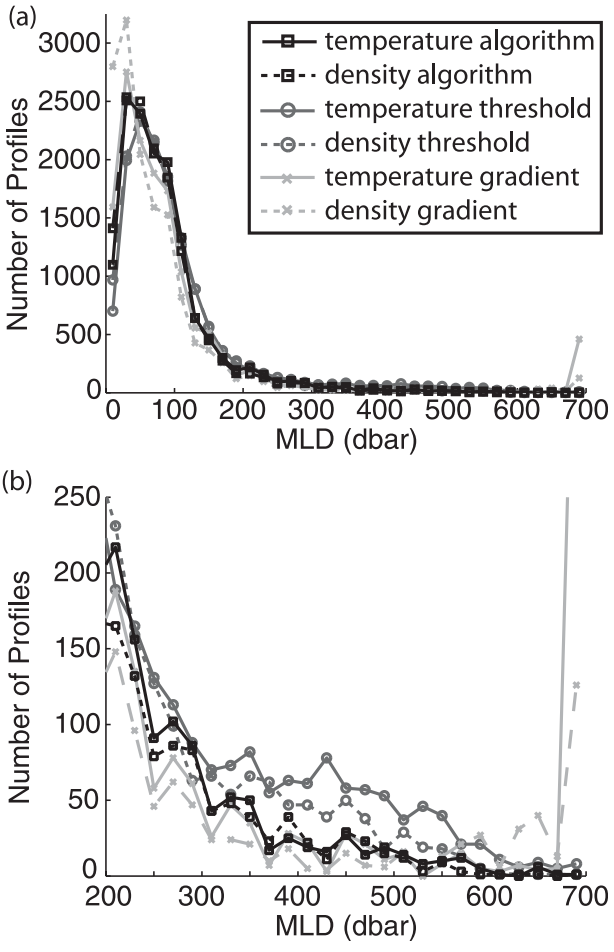

FIG. 12. Distribution of (a) all MLDs and (b) MLDs between 200 and 700 dbar found in the entire study region by six methods: temperature algorithm (solid black), density algorithm (dashed black), temperature threshold using de Boyer Montégut et al.'s (2004) criterion (solid dark gray), density threshold using de Boyer Montégut et al.'s (2004) criterion (dashed dark gray), temperature gradient (solid light gray; criterion of 0.005°C $dbar^{-1}$), and density gradient (dashed light gray; criterion of 0.0005 kg m^{-3} $dbar^{-1}$). The sawtooth pattern of the distribution in (b) is due to the depth sampling scheme of the Argo floats.

the MLD to be over 100 dbar deeper than the other methods. These anomalous density gradient MLDs do not fit with the general trend of the exact MLD.

In summer, the temperature algorithm, temperature threshold, and temperature gradient methods find similar MLDs. The MLD time series in Fig. 11b closely follow each other in the summer because of the strong temperature gradient beneath the mixed layer. The temperature algorithm is generally much more successful at finding winter MLDs than the temperature threshold and gradient methods. Judging the actual MLD visually, the temperature threshold method overestimates many MLDs during the winter of 2003 by approximately 200 dbar (Fig. 11b). Likewise, the temperature gradient method overestimates many MLDs during the winter of 2004. An example of this is given in Fig. 3a, in which the temperature is nearly uniform to a depth of 300 dbar. The MLD and density of this set of profiles are determined by salinity; the MLD is clearly 200 dbar in the salinity and density profiles. The temperature threshold and gradient methods estimate the MLD to be 375 and 360 dbar, respectively. The temperature algorithm identifies a small temperature protrusion at the base of the mixed layer and estimates an MLD of 220 dbar. This estimate is tied to a physical feature of the profile; compared to the temperature threshold and gradient MLDs, it is much closer to the actual MLD. The temperature algorithm's continued success at finding such features is evident in the similarity of its MLD to the density algorithm and density threshold MLDs (Figs. 11a,b).

c. *Southeast Pacific and southwest Atlantic comparison*

An analysis of the MLDs for the six methods from the southeast Pacific and southwest Atlantic Oceans confirms that the temperature algorithm improves on the temperature threshold and gradient methods and that the density algorithm offers a slight improvement over the other density methods. The MLD distributions of the six methods are plotted in Fig. 12. The temperature threshold method consistently overestimates deep MLDs relative to the other methods; it finds more MLDs between 250 and 600 dbar than any other method. The temperature and density gradient methods find the deepest MLDs: the temperature gradient method finds nearly 250 MLDs deeper than 700 dbar and the density gradient method finds 100 MLDs deeper than 700 dbar. None of the other methods finds mixed layers this deep. Figures 11a,b contain multiple examples of these deep gradient method MLDs. Both gradient methods, particularly density, are also prone to finding anomalously shallow MLDs; in Fig. 12a, both gradient methods find many more shallow MLDs (50 dbar or less) than the other methods.

In Figs. 13a,c, the scatter of temperature and density algorithm MLDs against the temperature and density threshold MLDs shows that the temperature and density algorithms generally find shallower MLDs than their threshold counterparts. The temperature threshold method systematically overestimates many MLDs relative to the temperature algorithm, forming a cluster of MLDs highlighted in Fig. 14a. Of these highlighted profiles, the temperature algorithm uses collocated temperature and temperature gradient maxima [Eq. (9)] to find the MLD for 75% of the profiles. This results in an

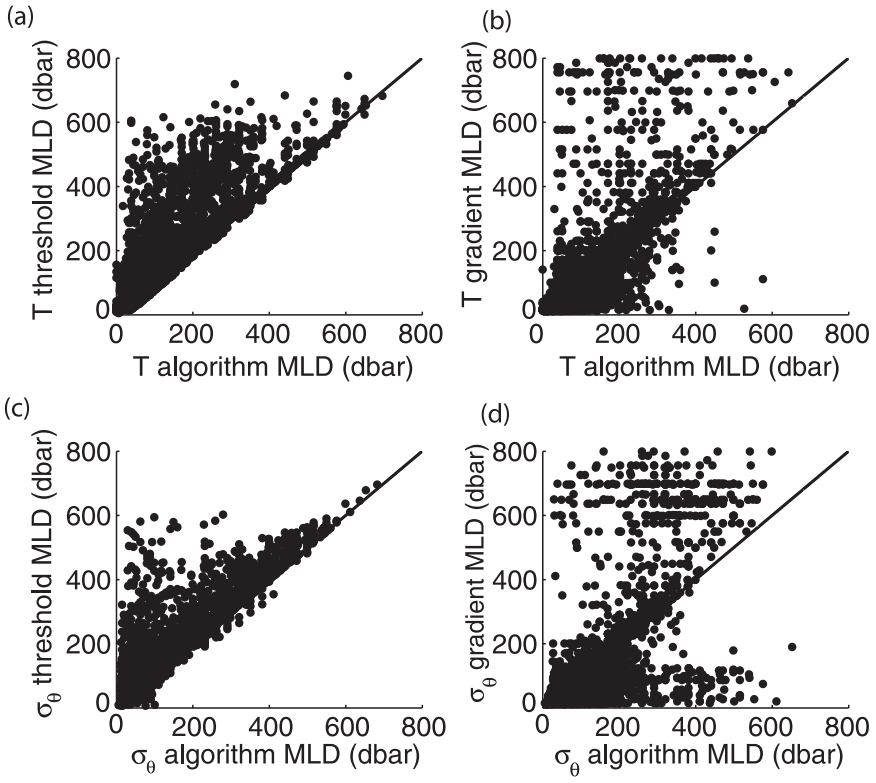

FIG. 13. Comparison of algorithm, threshold, and gradient MLD estimates from the study region: (a) temperature algorithm and temperature threshold, (b) temperature algorithm and temperature gradient, (c) density algorithm and density threshold, and (d) density algorithm and density gradient. The thin black line has a slope of 1.

average temperature algorithm MLD that better approximates the actual MLD than the average temperature threshold method, which overestimates the MLD by nearly 200 dbar (Fig. 14b).

Numerous examples of anomalously shallow and deep MLDs found by the temperature and density gradient methods are shown in Figs. 11a,b; Figs. 13b,d confirm the gradient methods' tendencies to find anomalous MLDs. The temperature gradient method finds more than 250 MLDs deeper than 700 dbar; these anomalously deep gradient MLDs correspond to temperature algorithm MLDs ranging from 25 to 600 dbar (Fig. 13b). The temperature gradient method's proclivity to overestimate the MLD in profiles with weak gradients beneath the mixed layer is also illustrated in Fig. 14b; for the subset of profiles, the average temperature gradient MLD is 250 dbar deeper than the average temperature algorithm MLD. Figure 13d illustrates the density gradient method's tendency to find anomalous MLDs; there is a large cluster of points corresponding to density gradient MLDs from 0 to 100 dbar and density algorithm MLDs varying from 0 to 600 dbar. Likewise, a similar cluster corresponds to density gradient MLDs deeper than 600 dbar and density algorithm MLDs between 25 and 600 dbar. Brainerd and Gregg (1995) found gradient methods to be less stable than threshold methods, a result mirrored in these distribution plots.

Figure 15 compares the density algorithm MLDs to the MLDs of the three temperature methods. Table 2 lists the means and standard deviations of the MLDs of the six methods, as well as the mean and standard deviation of the difference between the temperature methods MLDs and the density algorithm MLD. Together, these provide a means to evaluate the temperature methods relative to the density algorithm.

The cluster of deep temperature threshold MLDs highlighted in Fig. 14a is reproduced in Fig. 15a. There is no similar cluster in the scatter of density algorithm MLDs against the temperature algorithm MLDs (Fig. 15c). The temperature threshold method systematically overestimates deep MLDs, producing a mean MLD of 109 dbar. This mean MLD is 19 dbar deeper than the temperature algorithm mean MLD and 23 dbar deeper than the density algorithm mean MLD.

The temperature gradient method does not systematically overestimate the MLD relative to the density

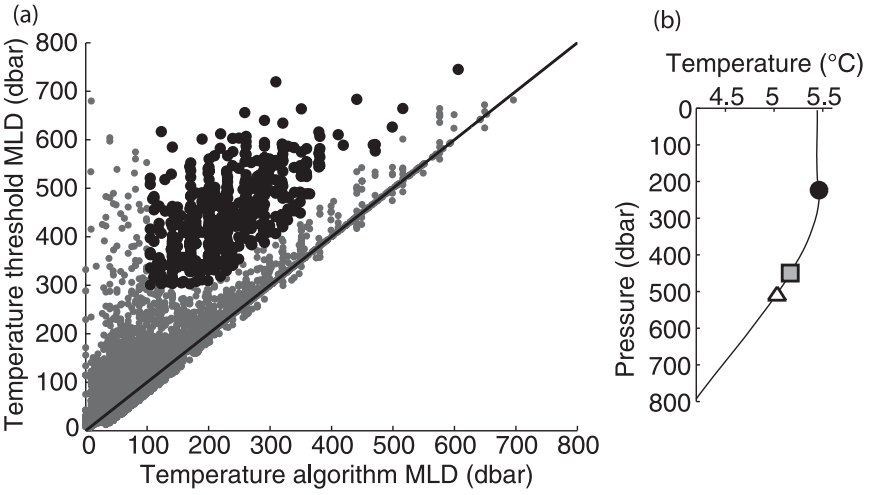

FIG. 14. (a) Comparison of temperature threshold and temperature algorithm MLDs, with a subset of MLDs highlighted by black dots, and (b) the average temperature profile for the subset of profiles. Three average MLD estimates are plotted in (b): the average temperature algorithm MLD (black circle), the average temperature gradient MLD (white triangle), and the average temperature threshold MLD (gray square). The thin black line in (a) has a slope of 1.

algorithm; rather, it identifies occasional anomalously deep MLDs compared to the density algorithm (Fig. 15b). These anomalously deep MLDs result in a mean temperature gradient MLD of 110 dbar (24 dbar deeper than the mean density algorithm MLD) and an MLD standard deviation of 161 dbar, which is much larger than any other method.

The temperature algorithm more closely tracks the density algorithm than the other temperature methods. The standard deviation of the difference between the temperature algorithm and the density algorithm MLDs is much smaller than the standard deviation of the difference between the density algorithm and the other temperature methods (Table 2). The temperature gradient method produces many MLDs similar to the temperature algorithm but is hampered by its tendency to find anomalously deep MLDs. The temperature threshold method routinely overestimates the depth of deep mixed layers.

d. Southern Ocean comparison

Expanding our analysis to algorithm and threshold MLD distributions for the entire Southern Ocean produces a more complex distribution of MLDs, though the general pattern is similar to the MLD distributions from the study region. Dong et al. (2008) produced a Southern Ocean MLD climatology from Argo float data and provided us with plots of the scatter of MLDs found by the temperature and density algorithms and threshold methods for the entire Southern Ocean (Fig. 16). As in the study region, the density methods produce very similar MLDs, though the threshold method tends to overestimate deep MLDs relative to the algorithm. The temperature methods exhibit much more scatter than

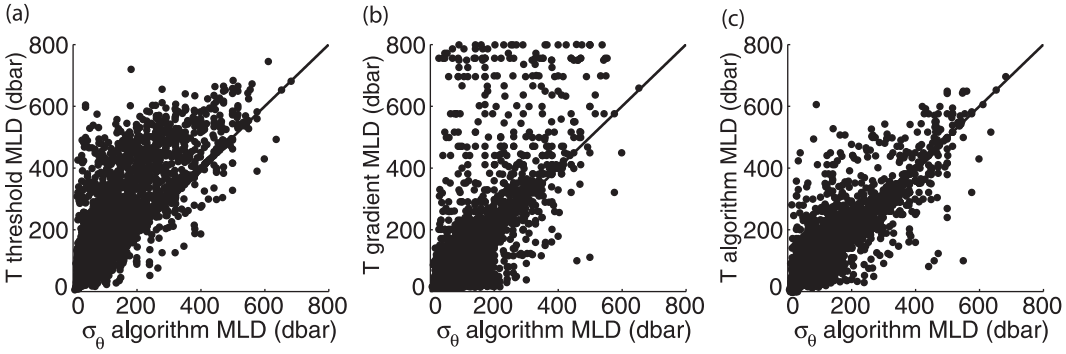

FIG. 15. Comparison of temperature (a) threshold, (b) gradient, and (c) algorithm MLDs to the density algorithm MLD. The thin black line has a slope of 1.

TABLE 2. MLD means and std devs (dbar) for the six methods: TA, TG, TT, DA, DG, and DT, as well as the means and std devs for the differences between DA and the three temperature methods.

	TA	TG	TT	DA	DG	DT	DA − TA	DA − TG	DA − TT
Mean	90	110	109	86	81	99	−4	−24	−23
Std dev	75	161	105	72	105	86	31	121	62

the density methods. In general, the temperature algorithm estimates shallower MLDs than the temperature threshold method; a cluster of MLDs similar to the cluster highlighted in Fig. 14a is also visible in the Southern Ocean distribution.

The algorithm's ability to identify physical features in the profiles allows it to track and identify the MLD more accurately than a traditional threshold method. Likewise, it is more stable than gradient methods. This accuracy makes the algorithm useful for identifying density-compensating and barrier layers. An accurate estimation of the mixed layer depth is important for ocean models that tune their turbulent mixing parameters to match observed ocean mixed layer depths (Noh et al. 2002). Because of its complexity, the algorithm is slower than threshold and gradient methods and it, like any MLD-finding method, is liable to be stumped by unusual profiles.

5. Application to SAMW mixed layers

One region of the ocean known for persistent deep winter mixed layers and water mass formation is immediately north of the ACC. The ACC encircles Antarctica as it flows eastward through the southern Pacific, Indian, and Atlantic Oceans. There are three fronts in the ACC associated with zonal jets in the current (Orsi et al. 1995). The deepest mixed layers in the Southern Ocean are associated with the northern side of the northernmost front, the Subantarctic Front (SAF). The waters defined and enclosed by these deep mixed layers were termed SAMW by McCartney (1977). AAIW, characterized by relatively low salinity, high oxygen, and low potential vorticity, is the densest, deepest, and freshest SAMW and is thought to form in the southeast Pacific just before the ACC enters the Drake Passage (McCartney 1977; England et al. 1993; Talley 1996; Hanawa and Talley 2001).

AAIW can be traced as a relatively low-salinity (34.4 psu) tongue throughout almost all of the Southern Hemisphere and the tropical oceans at about 1000 m depth (Deacon 1937). The global-scale heat and freshwater transports associated with AAIW's movement into the world's oceans reflect its relevance to studies of the earth's climate and of the ocean's global overturning circulation (Keeling and Stephens 2001; Pahnke and Zahn 2005). The SAMW and AAIW formation region is an ideal location to test methods for finding MLDs. The mixed layer exhibits great variability; in winter, the mixed layers north of the SAF can reach depths of 500 m and blend into deeper waters and remnant mixed layers. This makes determining the exact mixed layer

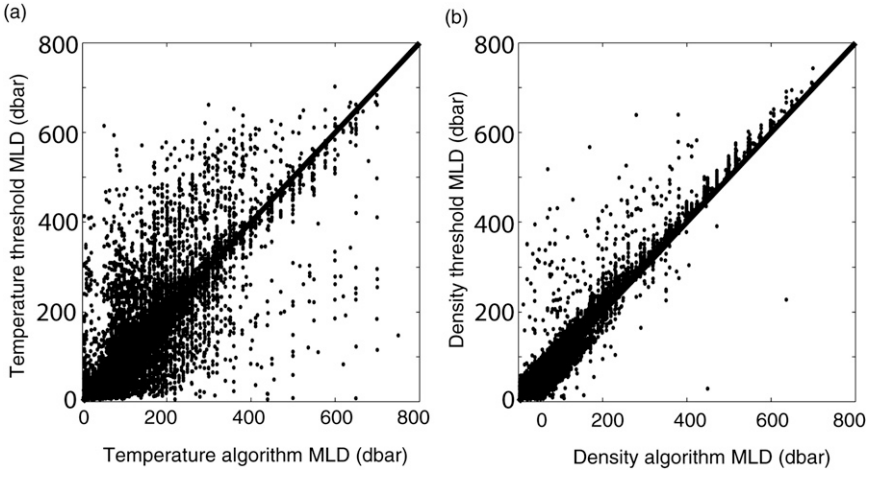

FIG. 16. Algorithm and threshold MLD estimates for the entire Southern Ocean for (a) the temperature algorithm and threshold and (b) the density algorithm and threshold. The thin black line has a slope of 1. These plots were provided by S. Dong (2006, personal communication).

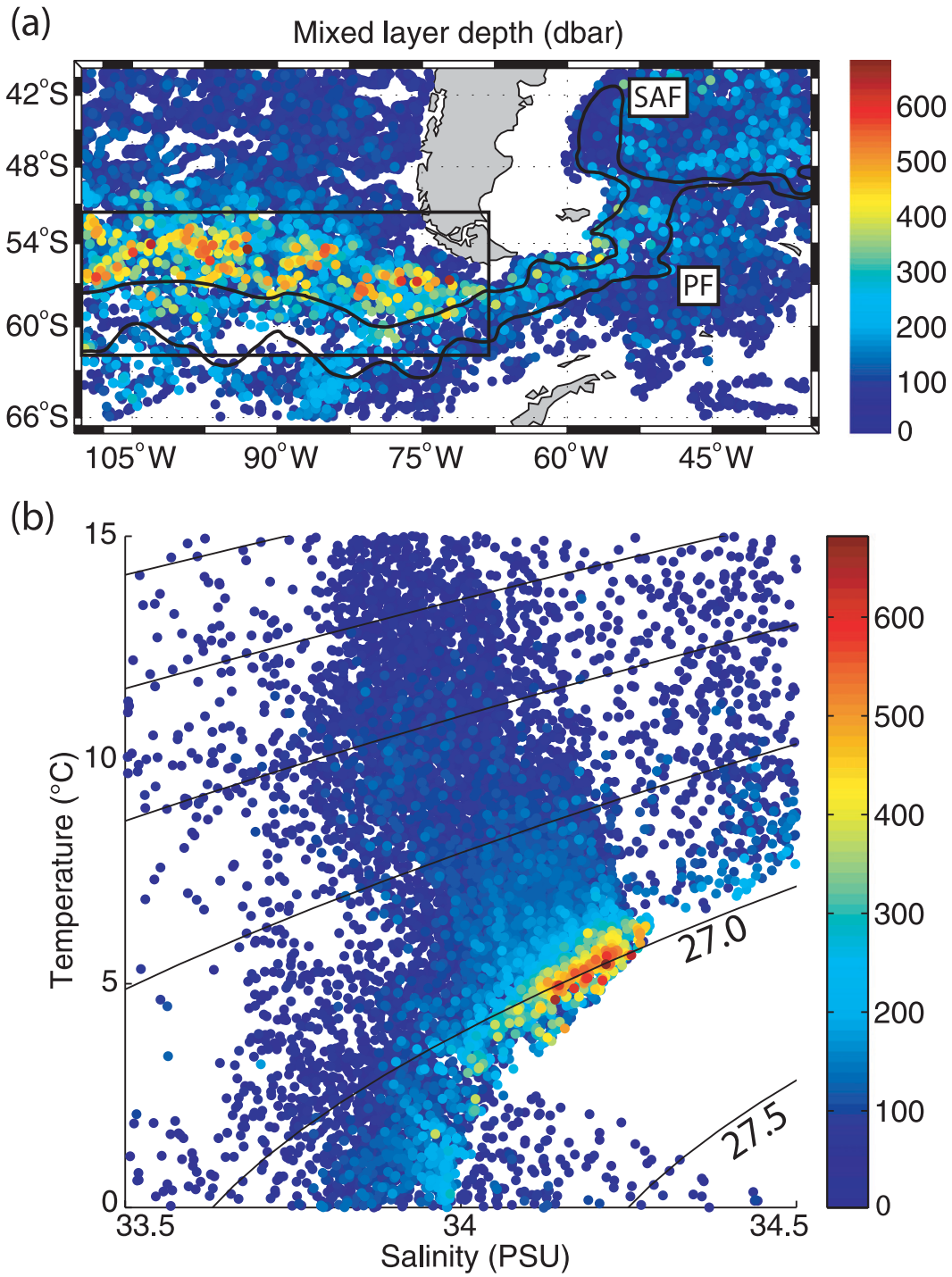

FIG. 17. The (a) MLD map and (b) mixed layer *T*–*S* diagram for the MLDs calculated by the density algorithm. The MLDs range from 0 dbar (blue) to 650 dbar (red). In (a), the SAF and Polar Front are represented by the solid lines (Orsi et al. 1995). Profiles from the boxed region (50°–62°S, 110°–68°W) are used in the MLD time series in Fig. 18 and the zonally averaged salinity section in Fig. 19. Each mixed layer's average temperature and salinity are plotted in (b); the color of each point corresponds to the MLD.

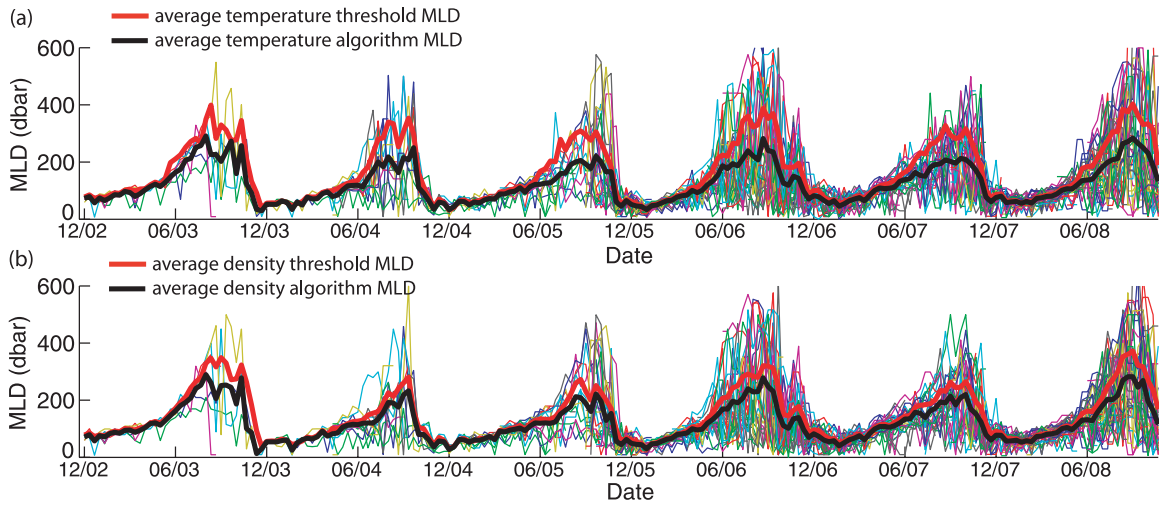

FIG. 18. Time series of MLDs (thin colored lines) derived by the (a) temperature and (b) density algorithms for floats within the region of deep mixed layers in the southeastern Pacific (50°–62°S, 110°–68°W). In (a), the average temperature algorithm MLD is plotted in black and the average temperature threshold MLD in red; (b) plots the average potential-density algorithm MLD in black and the average potential density threshold MLD in red.

difficult for many MLD-finding methods. Likewise, polar waters and summer stratification test methods' abilities to detect shallow mixed layers.

The algorithm identifies deep mixed layers, providing the locations; time of year; and temperature, salinity, and density characteristics of this oceanic process that has historically proven difficult to observe. The locations of SAMW formation, identified by deep mixed layers, are found by mapping all of the MLDs found by the density algorithm (Fig. 17). The deepest mixed layers are found in the southeast Pacific Ocean, immediately north of Orsi et al.'s (1995) climatological Subantarctic Front. The deepest MLDs are about 650 dbar, with numerous MLDs reaching 500 dbar. No regions of similarly deep mixed layers are found in the South Atlantic.

The density algorithm MLD map (Fig. 17) generally features a broader region of deep mixed layers compared to four MLD climatologies (not shown). The 95% oxygen saturation depth has been used by Talley (1999) as a proxy for the MLD. Using Antonov et al.'s (2006) 95% oxygen saturation depth as an MLD proxy produces MLDs of roughly the same depth range as the algorithm, but the climatology's region of deep MLDs is more localized and centered at 53°S and 92°W. Levitus and Boyer's (1994) MLD climatology shows MLDs of 1000 m, far deeper than anything found by Argo in the study region. Their deepest MLDs are also localized and centered at 52°S and 87°W. The deepest MLDs of de Boyer Montégut et al.'s (2004) climatology reach 450 m at 90°W and do not extend farther west. Kara et al. (2003) used Levitus and Boyer's (1994) density in constructing their climatology. The spatial distribution of their MLDs is similar to the density algorithm, but their MLDs reach 800 m, considerably deeper than any mixed layers found by the density algorithm.

The temperature, salinity, and potential-density characteristics of the deep mixed layers are identified with a *T–S* diagram (Fig. 17). The deepest mixed layers have average potential densities of approximately 27 kg m^{-3}, salinities of 34.1–34.2 psu, and temperatures of 4°–5°C.

Figure 18 plots the MLD time series of the floats in the area of the Pacific with deep mixed layers. This region, from 50° to 62°S and from 110° to 68°W, is boxed in Fig. 17. The deepest MLDs occur in August and September. The temporal extent of the deep MLDs was greater for the 2003 winter than for any other. The mixed layers gradually deepen over the course of six months leading up to August and September, after which they quickly restratify. The average MLD reached in winter is approximately 300 dbar, though individual floats record MLDs exceeding 650 dbar. As shown in section 4, the threshold methods overestimate the MLD relative to the algorithms. In particular, the temperature hreshold method produces winter periods of deep mixed layers that are of earlier onset, greater duration, and greater depth than the temperature algorithm (Fig. 18a).

To examine how the deep mixed layers relate to AAIW, the zonal average salinity for the Pacific study region during winter is plotted in Fig. 19. From this average section, the low-salinity water mass at middepth (500–600 dbar in Fig. 19, between the 27.0 and 27.1 kg m^{-3} isopycnals) can be traced to a surface density outcropping between 58° and 60°S. The region of deep mixed

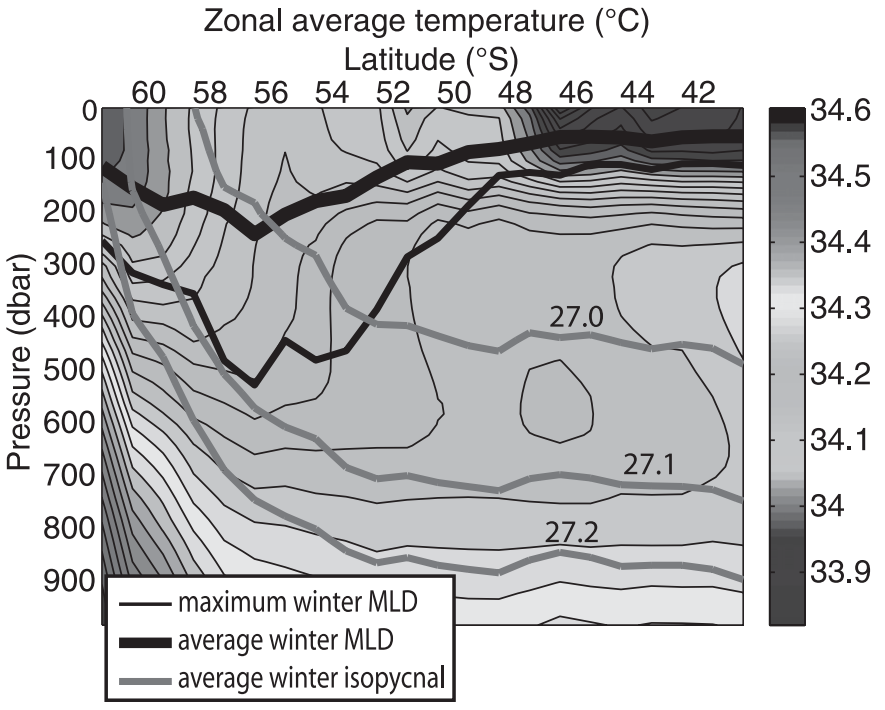

FIG. 19. Zonally averaged salinity of all profiles collected in the southeastern Pacific region (Fig. 17) during winter. The study period covers six winters, identified as intervals of deep mixed layers running from mid-June to early November for 2003–08. An Akima spline was used to interpolate each profile to uniform vertical spacing, at which point they were averaged into 1° latitude bins. The salinity is contoured at 0.025-psu intervals. The bold black line is the average winter MLD based on the density algorithm MLD of each profile. The thin black line, representing the maximum winter MLD in the 1° bin, is the average of the five deepest MLDs, again determined by the sensity algorithm. Three potential contours (σ_θ = 27.0, 27.1, 27.2 kg m^{-3}) are plotted in gray.

layers corresponds to a sea surface salinity maximum between 54° and 57°S. On average, these deep winter mixed layers in the southeast Pacific Ocean appear to penetrate into the low-salinity layer at 56°S and inject low-salinity water of the correct salinity, density class, and depth as AAIW into the ocean interior.

6. Summary

A new algorithm was developed to find the MLD of individual Argo ocean profiles. The algorithm fits straight lines to the mixed layer and thermocline, searches for subsurface property anomalies, and incorporates threshold and gradient methods to find the MLD. The temperature and density algorithms tend to find shallower MLDs than their threshold counterparts. The temperature algorithm MLD nearly matches the density algorithm MLD. In the study region, the temperature algorithm offers a marked improvement over a temperature threshold method using the criterion of de Boyer Montégut et al. (2004); the temperature threshold method frequently overestimates winter MLDs by nearly 200 dbar for profiles in which the temperature algorithm successfully identifies temperature anomalies at the base of the mixed layer. The temperature algorithm is preferred over the temperature gradient method because of the gradient method's tendency to find anomalously deep MLDs. The density gradient method also produces many anomalous MLDs. The algorithm was used to investigate the formation of SAMW and AAIW in the southeast Pacific and southwest Atlantic Oceans. We find that the deepest MLDs routinely reach 500 dbar and occur north of the Orsi et al. (1995) mean SAF in the southeastern Pacific Ocean. Within the Pacific study region, the deepest winter mixed layers occur in August and September at 57°S and are concurrent with the subsurface salinity minimum, a signature of AAIW.

Acknowledgments. NSF Ocean Sciences Division Grant OCE-0327544 supported this work. Harold Freeland of IOS, Sidney, BC, pioneered the deployment of

Argo floats in the southeast Pacific. Shenfu Dong kindly provided us with plots of algorithm and threshold MLDs for the entire Southern Ocean. Sharon Escher helped refine the algorithm's coding. Three anonymous reviewers provided many useful comments that greatly improved the manuscript.

REFERENCES

Antonov, J. A., R. A. Locarnini, T. P. Boyer, H. E. Garcia, and A. Mishonov, 2006: *Salinity*. Vol. 2, *World Ocean Atlas 2005,* NOAA Atlas NESDIS 62, 50 pp.

Brainerd, K. E., and M. C. Gregg, 1995: Surface mixed and mixing layer depths. *Deep-Sea Res. I,* **42,** 1521–1543.

Chen, D., A. J. Busalacchi, and L. M. Rothstein, 1994: The roles of vertical mixing, solar radiation, and wind stress in a model simulation of the sea surface temperature seasonal cycle in the tropical Pacific Ocean. *J. Geophys. Res.,* **99,** 20 345–20 359.

Chereskin, T. K., and D. Roemmich, 1991: A comparison of measured and wind-derived Ekman transport at 11°N in the Atlantic Ocean. *J. Phys. Oceanogr.,* **21,** 869–878.

Chu, P. C., Q. Wang, and R. H. Bourke, 1999: A geometric model for the Beaufort/Chukchi Sea thermohaline structure. *J. Atmos. Oceanic Technol.,* **16,** 613–632.

Deacon, G. E. R., 1937: The hydrology of the Southern Ocean. *Discovery Rep.,* **15,** 1–124.

de Boyer Montégut, C., G. Madec, A. S. Fischer, A. Lazar, and D. Iudicone, 2004: Mixed layer depth over the global ocean: An examination of profile data and a profile-based climatology. *J. Geophys. Res.,* **109,** C12003, doi:10.1029/2004JC002378.

Dong, S., J. Sprintall, S. T. Gille, and L. Talley, 2008: Southern Ocean mixed-layer depth from Argo float profiles. *J. Geophys. Res.,* **113,** C06013, doi:10.1029/2006JC004051.

England, M. H., J. S. Godfrey, A. C. Hirst, and M. Tomczak, 1993: The mechanism for Antarctic Intermediate Water renewal in a world ocean model. *J. Phys. Oceanogr.,* **23,** 1553–1560.

Hanawa, K., and L. D. Talley, 2001: Mode waters. *Ocean Circulation and Climate,* G. Siedler, J. Church, and J. Gould, Eds., Academic Press, 373–386.

Kara, A. B., P. A. Rochford, and H. E. Hurlburt, 2000: An optimal definition for ocean mixed layer depth. *J. Geophys. Res.,* **105,** 16 803–16 821.

——, ——, and ——, 2003: Mixed layer depth variability over the global ocean. *J. Geophys. Res.,* **108,** 3079, doi:10.1029/2000JC000736.

Keeling, R. F., and B. B. Stephens, 2001: Antarctic sea ice and the control of Pleistocene climate instability. *Paleoceanography,* **16,** 112–131, doi:10.1029/2000PA000529.

Lavender, K. L., R. E. Davis, and W. B. Owens, 2002: Observations of open-ocean deep convection in the Labrador Sea from subsurface floats. *J. Phys. Oceanogr.,* **32,** 511–526.

Levitus, S., R. Burgett, and T. P. Boyer, 1994: *Salinity*. Vol. 3, *World Ocean Atlas 1994,* NOAA Atlas NESDIS 3, 99 pp.

Lorbacher, K., D. Dommenget, P. P. Niiler, and A. Köhl, 2006: Ocean mixed layer depth: A subsurface proxy of ocean-atmosphere variability. *J. Geophys. Res.,* **111,** C07010, doi:10.1029/2003JC002157.

Lukas, R., and E. Lindstrom, 1991: The mixed layer of the western equatorial Pacific Ocean. *J. Geophys. Res.,* **96,** 3343–3358.

Marshall, J., and F. Schott, 1999: Open-ocean convection: Observations, theory, and models. *Rev. Geophys.,* **37,** 1–64.

McCartney, M. S., 1977: Subantarctic Mode Water. *A Voyage of Discovery: George Deacon 70th Anniversary Volume,* M. V. Angel, Ed., Pergamon, 103–119.

Monterey, G., and S. Levitus, 1997: *Seasonal Variability of Mixed Layer Depth for the World Ocean*. NOAA Atlas NESDIS 14, 96 pp.

Noh, Y., C. J. Jang, T. Yamagata, P. C. Chu, and C. H. Kim, 2002: Simulation of more realistic upper-ocean processes from an OGCM with a new ocean mixed layer model. *J. Phys. Oceanogr.,* **32,** 1284–1307.

Ohlmann, J. C., D. A. Siegel, and C. Gautier, 1996: Ocean mixed layer radiant heating and solar penetration: A global analysis. *J. Climate,* **9,** 2265–2280.

Oka, E., L. D. Talley, and T. Suga, 2007: Temporal variability of winter mixed layer in the mid-to high-latitude North Pacific. *J. Oceanogr.,* **63,** 293–307.

Orsi, A. H., T. Whitworth, and W. D. Nowlin, 1995: On the meridional extent and fronts of the Antarctic Circumpolar Current. *Deep-Sea Res. I,* **42,** 641–673.

Pahnke, K., and R. Zahn, 2005: Millennial-scale Antarctic Intermediate Water variability over the past 340,000 years as recorded by benthic foraminiferal δ13C in the mid-depth southwest Pacific. Extended Abstracts, *Spring Meeting,* New Orleans, LA, Amer. Geophys. Union, A4+.

Roemmich, D., and Coauthors, 2001: Argo: The global array of profiling floats. *Observing the Oceans in the 21st Century,* K. J. Koblinksy and N. R. Smith, Eds., Bureau of Meteorology, 604 pp.

Sprintall, J., and M. Tomczak, 1992: Evidence of the barrier layer in the surface layer of the tropics. *J. Geophys. Res.,* **97,** 7305–7316.

——, and D. Roemmich, 1999: Characterizing the structure of the surface layer in the Pacific Ocean. *J. Geophys. Res.,* **104,** 23 297–23 311.

Talley, L. D., 1996: Antarctic Intermediate Water in the South Atlantic. *The South Atlantic: Present and Past Circulation,* G. Wefer et al., Eds., Springer-Verlag, 219–238.

——, 1999: Some aspects of ocean heat transport by the shallow, intermediate and deep overturning circulations. *Mechanisms of Global Climate Change at Millennial Time Scales, Geophys. Monogr.,* Vol. 112, Amer. Geophys. Union, 1–22.

Thomson, R. E., and I. V. Fine, 2003: Estimating mixed layer depth from oceanic profile data. *J. Atmos. Oceanic Technol.,* **20,** 319–329.

Tsuchiya, M., and L. D. Talley, 1998: A Pacific hydrographic section at 88°W: Water-property distribution. *J. Geophys. Res.,* **103,** 12 899–12 918.